Measurement of the CP Asymmetry in $B^+ \to K^+ \mu^+ \mu^-$ Decays

R. Aaij *et al.**
(LHCb Collaboration)

(Received 7 August 2013; published 7 October 2013)

A measurement of the CP asymmetry in $B^+ \to K^+ \mu^+ \mu^-$ decays is presented using pp collision data, corresponding to an integrated luminosity of 1.0 fb^{-1}, recorded by the LHCb experiment during 2011 at a center-of-mass energy of 7 TeV. The measurement is performed in seven bins of $\mu^+\mu^-$ invariant mass squared in the range $0.05 < q^2 < 22.00\ \mathrm{GeV}^2/c^4$, excluding the J/ψ and $\psi(2S)$ resonance regions. Production and detection asymmetries are corrected for using the $B^+ \to J/\psi K^+$ decay as a control mode. Averaged over all the bins, the CP asymmetry is found to be $\mathcal{A}_{CP} = 0.000 \pm 0.033\,(\mathrm{stat}) \pm 0.005\,(\mathrm{syst}) \pm 0.007\ (J/\psi K)$, where the third uncertainty is due to the CP asymmetry of the control mode. This is consistent with the standard model prediction.

DOI: 10.1103/PhysRevLett.111.151801 PACS numbers: 13.20.He, 11.30.Er, 12.15.Mm, 12.60.Jv

The rare decay $B^+ \to K^+ \mu^+ \mu^-$ is a flavor-changing neutral current process mediated by electroweak loop (penguin) and box diagrams. The absence of tree-level diagrams for the decay results in a small value of the standard model (SM) prediction for the branching fraction, which is supported by a measurement of $(4.36 \pm 0.23) \times 10^{-7}$ [1]. Physics processes beyond the SM that may enter via the loop and box diagrams could have large effects on observables of the decay. Examples include the decay rate, the $\mu^+\mu^-$ forward-backward asymmetry [1–3], and the CP asymmetry [2,4], as functions of the $\mu^+\mu^-$ invariant mass squared (q^2).

The CP asymmetry is defined as

$$\mathcal{A}_{CP} = \frac{\Gamma(B^- \to K^- \mu^+ \mu^-) - \Gamma(B^+ \to K^+ \mu^+ \mu^-)}{\Gamma(B^- \to K^- \mu^+ \mu^-) + \Gamma(B^+ \to K^+ \mu^+ \mu^-)}, \qquad (1)$$

where Γ is the decay rate of the mode. This asymmetry is predicted to be of order 10^{-4} in the SM [5] but can be significantly enhanced in models beyond the SM [6]. Current measurements including the dielectron mode $\mathcal{A}_{CP}(B \to K^+ \ell^+ \ell^-)$ from *BABAR* and Belle give -0.03 ± 0.14 and 0.04 ± 0.10, respectively [2,4], and are consistent with the SM. The CP asymmetry has already been measured at LHCb in $B^0 \to K^{*0} \mu^+ \mu^-$ decays [7], $\mathcal{A}_{CP} = -0.072 \pm 0.040$. Assuming that contributions beyond the SM are independent of the flavor of the spectator quark, $\mathcal{A}_{CP}$ should be similar for both $B^+ \to K^+ \mu^+ \mu^-$ and $B^0 \to K^{*0} \mu^+ \mu^-$ decays.

In this Letter, a measurement of $\mathcal{A}_{CP}$ in $B^+ \to K^+ \mu^+ \mu^-$ decays is presented using pp collision data, corresponding to an integrated luminosity of 1.0 fb^{-1}, recorded at a center-of-mass energy of 7 TeV at LHCb in 2011. The inclusion of charge conjugate modes is implied throughout unless explicitly stated.

The LHCb detector [8] is a single-arm forward spectrometer covering the pseudorapidity range $2 < \eta < 5$, designed for the study of particles containing b or c quarks. The detector includes a high-precision tracking system consisting of a silicon-strip vertex detector surrounding the pp interaction region, a large-area silicon-strip detector located upstream of a dipole magnet with a bending power of about 4 Tm, and three stations of silicon-strip detectors and straw drift tubes placed downstream. The combined tracking system provides a momentum measurement with relative uncertainty that varies from 0.4% at 5 GeV$/c$ to 0.6% at 100 GeV$/c$, and impact parameter (IP) resolution of 20 μm for tracks with high transverse momentum (p_T). Charged hadrons are identified using two ring-imaging Cherenkov detectors [9]. Muons are identified by a system composed of alternating layers of iron and multiwire proportional chambers [10].

Samples of simulated events are used to determine the efficiency of selecting $B^+ \to K^+ \mu^+ \mu^-$ signal events and to study certain backgrounds. In the simulation, pp collisions are generated using PYTHIA 6.4 [11] with a specific LHCb configuration [12]. Decays of hadronic particles are described by EVTGEN [13], in which final-state radiation is generated using PHOTOS [14]. The interaction of the generated particles with the detector and its response are implemented using the GEANT4 toolkit [15] as described in Ref. [16]. The simulated samples are corrected to reproduce the data distributions of the B^+ meson p_T and vertex χ^2, the track χ^2 of the kaon, as well as the detector IP resolution, particle identification, and momentum resolution.

Candidate events are first required to pass a hardware trigger, which selects muons with $p_T > 1.48$ GeV$/c$ [17]. In the subsequent software trigger, at least one of the final-state particles is required to have $p_T > 1.0$ GeV$/c$ and IP $>$100 μm with respect to all primary pp interaction

*Full author list given at end of the article.

vertices (PVs) in the event. Finally, the tracks of two or more of the final-state particles are required to form a vertex that is displaced from the PVs.

An initial selection is applied to the $B^+ \to K^+\mu^+\mu^-$ candidates to enhance signal decays and suppress combinatorial background. Candidate B^+ mesons must satisfy requirements on their direction and flight distance, to ensure consistency with originating from the PV. The decay products must pass criteria regarding the $\chi^2_{\rm IP}$, where $\chi^2_{\rm IP}$ is defined as the difference in χ^2 of a given PV reconstructed with and without the considered particle. There is also a requirement on the vertex χ^2 of the $\mu^+\mu^-$ pair. All the tracks are required to have $p_T > 250$ MeV$/c$.

Additional background rejection is achieved by using a boosted decision tree [18] that implements the AdaBoost algorithm [19]. The boosted decision tree uses the p_T and $\chi^2_{\rm IP}$ of the muons and the B^+ meson candidate, as well as the decay time, vertex χ^2, and flight direction of the B^+ candidate and the $\chi^2_{\rm IP}$ of the kaon. Data, corresponding to an integrated luminosity of 0.1 fb^{-1}, are used to optimize this selection, leaving 0.9 fb^{-1} for the determination of $\mathcal{A}_{CP}$.

Following the multivariate selection, candidate events pass several requirements to remove specific sources of background. Particle identification criteria are applied to kaon candidates to reduce the number of pions incorrectly identified as kaons. Candidates with $\mu^+\mu^-$ invariant mass in the ranges $2.95 < m_{\mu\mu} < 3.18$ GeV$/c^2$ and $3.59 < m_{\mu\mu} < 3.77$ GeV$/c^2$ are removed to reject backgrounds from tree level $B^+ \to J/\psi(\to \mu^+\mu^-)K^+$ and $B^+ \to \psi(2S)(\to \mu^+\mu^-)K^+$ decays. Those in the first range are selected as $B^+ \to J/\psi K^+$ decays, which are used as a control sample. If $m_{K\mu\mu} < 5.22$ GeV$/c^2$, the vetoes are extended downwards by 0.25 and 0.19 GeV$/c^2$, respectively, to remove the radiative tails of the resonant decays. If $5.35 < m_{K\mu\mu} < 5.50$ GeV$/c^2$, the vetoes are extended upwards by 0.05 GeV$/c^2$ to remove misreconstructed resonant candidates that appear at large $m_{\mu\mu}$ and $m_{K\mu\mu}$. Further vetoes are applied to remove $B^+ \to J/\psi K^+$ events in which the kaon and a muon have been swapped and contributions from decays involving charm mesons such as $B^+ \to \bar{D}^0(\to K^+\pi^-)\pi^+$ where both pions are misidentified as muons. After these selection requirements have been applied, there are two sources of background that are difficult to distinguish from the signal. These are $B^+ \to K^+\pi^+\pi^-$ and $B^+ \to \pi^+\mu^+\mu^-$ decays, which both contribute at the level of 1% of the signal yield. These peaking backgrounds are accounted for during the analysis.

In order to perform a measurement of $\mathcal{A}_{CP}$, the production and detection asymmetries associated with the measurement must be considered. The raw measured asymmetry is, to first order,

$$\mathcal{A}_{\rm RAW} = \mathcal{A}_{CP} + \mathcal{A}_P + \mathcal{A}_D, \qquad (2)$$

where the production and detection asymmetries are defined as

$$\mathcal{A}_P \equiv [R(B^-) - R(B^+)]/[R(B^-) + R(B^+)], \qquad (3)$$

$$\mathcal{A}_D \equiv [\epsilon(K^-) - \epsilon(K^+)]/[\epsilon(K^-) + \epsilon(K^+)], \qquad (4)$$

where R and ϵ represent the B meson production rate and kaon detection efficiency, respectively. The detection asymmetry has two components: one due to the different interactions of positive and negative kaons with the detector material, and a left-right asymmetry due to particles of different charges being deflected to opposite sides of the detector by the magnet. The component of the detection asymmetry from muon reconstruction is small and neglected. Since the LHCb experiment reverses the magnetic field, about half of the data used in the analysis is taken with each polarity. Therefore, an average of the measurements with the two polarities is used to suppress significantly the second effect. To account for both the detection and production asymmetries, the decay $B^+ \to J/\psi K^+$ is used, which has the same final-state particles as $B^+ \to K^+\mu^+\mu^-$ and very similar kinematic properties. The CP asymmetry in $B^+ \to J/\psi K^+$ decays has been measured as $(1 \pm 7) \times 10^{-3}$ [20,21]. Neglecting the difference in the final-state kinematic properties of the kaon, the production and detection asymmetries are the same for both modes, and the value of the CP asymmetry can be obtained via

$$\mathcal{A}_{CP} = \mathcal{A}_{\rm RAW}(K\mu\mu) - \mathcal{A}_{\rm RAW}(J/\psi K) + \mathcal{A}_{CP}(J/\psi K). \qquad (5)$$

Differences in the kinematic properties are accounted for by a systematic uncertainty.

In the data set, approximately 1330 $B^+ \to K^+\mu^+\mu^-$ and 218 000 $B^+ \to J/\psi K^+$ signal decays are reconstructed. To measure any variation in $\mathcal{A}_{CP}$ as a function of q^2, which improves the sensitivity of the measurement to physics beyond the SM, the $B^+ \to K^+\mu^+\mu^-$ data set is divided into the seven q^2 bins used in Ref. [1]. The measurement is also made in a bin of $1 < q^2 < 6$ GeV$^2/c^4$, which is of particular theoretical interest. To determine the number of B^+ decays in each bin, a simultaneous unbinned maximum likelihood fit is performed to the invariant mass distributions of the $B^+ \to K^+\mu^+\mu^-$ and $B^+ \to J/\psi K^+$ candidates in the range $5.10 < m_{K\mu\mu} < 5.60$ GeV$/c^2$. The signal shape is parametrized by a Cruijff function [22], and the combinatorial background is described by an exponential function. All parameters of the signal and combinatorial background are allowed to vary freely in the fit. Additionally, there is background from partially reconstructed decays such as $B^0 \to K^{*0}(\to K^+\pi^-)\mu^+\mu^-$ or $B^0 \to J/\psi K^{*0}(\to K^+\pi^-)$ where the pion is undetected. For the $B^+ \to K^+\mu^+\mu^-$ distribution, these decays are fitted by an ARGUS function [23] convolved with a Gaussian function to account for detector resolution. For the $B^+ \to J/\psi K^+$ decays, the partially reconstructed background is modeled by another Cruijff function. The shapes of the peaking backgrounds, due to $B^+ \to K^+\pi^+\pi^-$ and $B^+ \to \pi^+\mu^+\mu^-$ decays, are taken from fits to simulated events.

In each q^2 bin, the $B^+ \to J/\psi K^+$ and $B^+ \to K^+\mu^+\mu^-$ data sets are divided according to the charge of the B^+ meson and magnet polarity, providing eight distinct subsets. These are fitted simultaneously with the parameters of the signal Cruijff function common for all eight subsets. For each subset, the only independent fitting parameters are the combined yield of the B^+ and B^- decays and the values of $\mathcal{A}_{\rm RAW}$ for the signal, control, and background modes for each magnet polarity. The fits to the invariant mass distributions of the $B^+ \to K^+\mu^+\mu^-$ candidates in the full q^2 range are shown in Fig. 1.

The value of $\mathcal{A}_{CP}$ for each magnet polarity is determined from Eq. (5), and an average with equal weights is taken to obtain a single value for the q^2 bin. To obtain the final value of $\mathcal{A}_{CP}$ for the full data set, an average is taken of the values in each q^2 bin, weighted according to the signal efficiency and the number of $B^+ \to K^+\mu^+\mu^-$ decays in the bin

$$\mathcal{A}_{CP} = \frac{\sum_{i=1}^{7}(N_i \mathcal{A}_{CP}^{i})/\epsilon_i}{\sum_{i=1}^{7} N_i/\epsilon_i}, \quad (6)$$

where N_i, ϵ_i, and $\mathcal{A}_{CP}^{i}$ are the signal yield, signal efficiency, and the fitted value of the CP asymmetry in the ith q^2 bin.

Several assumptions are made about the backgrounds. The partially reconstructed background is assumed to exhibit no CP asymmetry. For $B^+ \to \pi^+\mu^+\mu^-$, $\mathcal{A}_{CP}$ is also assumed to be zero [24]. For the $B^+ \to K^+\pi^+\pi^-$ decay, $\mathcal{A}_{CP}$ in each q^2 bin is taken from a recent LHCb measurement [25]. The effect of these assumptions on the result is investigated as a systematic uncertainty.

Various sources of systematic uncertainty are considered. The analysis relies on the assumption that the $B^+ \to K^+\mu^+\mu^-$ and $B^+ \to J/\psi K^+$ decays have the same final-state kinematic distributions, so that the relation in Eq. (5) is exact. To estimate the bias associated with this assumption, the kinematic distributions of $B^+ \to J/\psi K^+$ decays are reweighted to match those of $B^+ \to K^+\mu^+\mu^-$, and the value of $\mathcal{A}_{\rm RAW}$ is recalculated. The variables used are the momentum, p_T, and pseudorapidity of the B^+ and K^+ mesons, as well as the B^+ decay time and the position of the kaon in the detector. The difference between the two values of $\mathcal{A}_{\rm RAW}$ for each variable is taken as the systematic uncertainty. The total systematic uncertainty associated with the different kinematic behavior of the two decays in each q^2 bin is calculated by adding each individual contribution in quadrature.

The choice of fit model also introduces systematic uncertainties. The fit is repeated using a different signal model, replacing the Cruijff function with the sum of two Crystal Ball functions [26] that have the same mean and tail parameters but different Gaussian widths. The

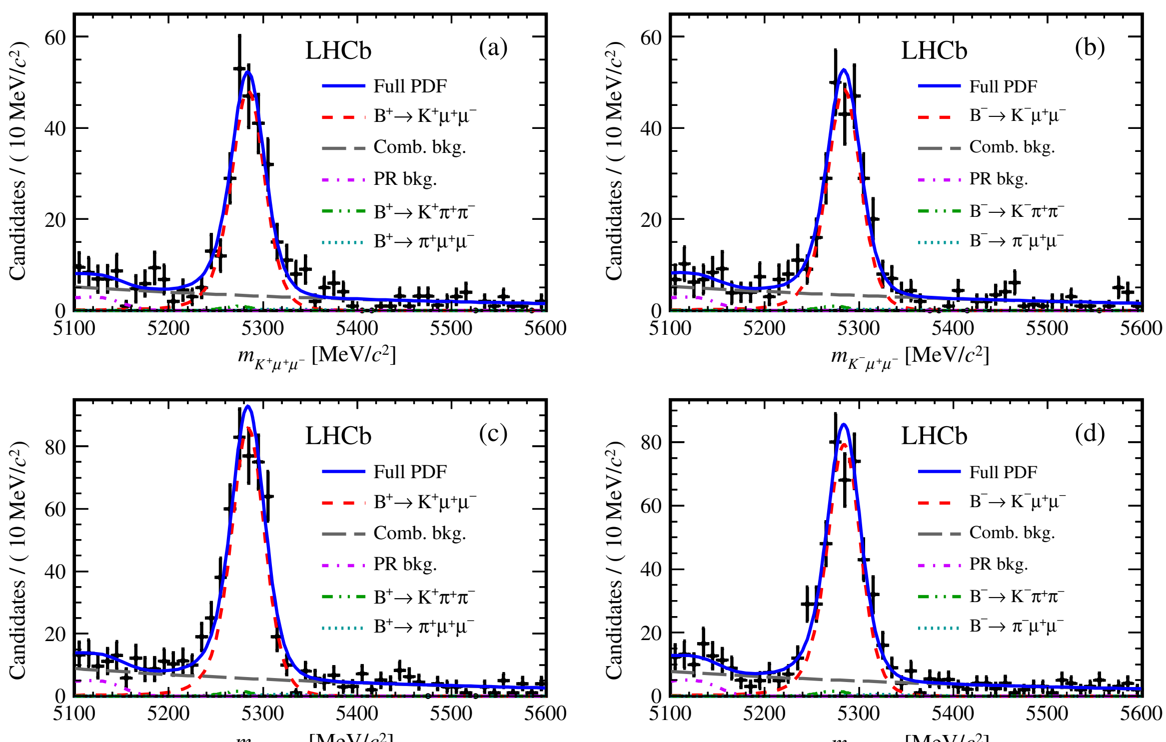

FIG. 1 (color online). Invariant mass distributions of $B^+ \to K^+\mu^+\mu^-$ candidates for the full q^2 range. The results of the unbinned maximum likelihood fits are shown with solid blue lines. Also shown are the signal component (short-dashed red line), the combinatorial background (long-dashed gray line), and the partially reconstructed background (dot-dashed magenta line). The peaking backgrounds $B^+ \to K^+\pi^+\pi^-$ (double-dot-dashed green line) and $B^+ \to \pi^+\mu^+\mu^-$ (dotted teal line) are also shown under the signal peak. The four data sets are (a) B^+ and (b) B^- for one magnet polarity and (c) B^+ and (d) B^- for the other.

TABLE I. Systematic uncertainties on $\mathcal{A}_{CP}$ from noncanceling asymmetries arising from kinematic differences between $B^+ \to J/\psi K^+$ and $B^+ \to K^+\mu^+\mu^-$ decays and fit uncertainties arising from the choice of signal shape, mass fit range, and combinatorial background shape, and from the treatment of the asymmetries in the $B^+ \to \pi^+\mu^+\mu^-$ and partially reconstructed (PR) backgrounds. The total is the sum in quadrature of each component.

q^2 bin (GeV^2/c^4)	Residual asymmetries	Signal shape	Mass range	Combinatorial shape	$\mathcal{A}_{CP}$ in $B^+ \to \pi^+\mu^+\mu^-$	$\mathcal{A}_{CP}$ in PR	Total
$0.05 < q^2 < 2.00$	0.005	0.005	0.002	0.002	0.004	0.002	0.008
$2.00 < q^2 < 4.30$	0.004	0.001	0.005	0.009	0.005	0.001	0.012
$4.30 < q^2 < 8.68$	0.001	0.001	0.001	0.001	0.005	0.002	0.005
$10.09 < q^2 < 12.86$	0.003	0.005	0.023	0.003	0.003	0.001	0.024
$14.18 < q^2 < 16.00$	0.006	0.001	0.004	0.003	<0.001	0.001	0.008
$16.00 < q^2 < 18.00$	0.005	0.007	0.017	<0.001	<0.001	0.001	0.019
$18.00 < q^2 < 22.00$	0.008	0.001	0.014	<0.001	0.001	0.001	0.016
Weighted average	0.001	<0.001	0.003	0.001	0.003	<0.001	0.005
$1.00 < q^2 < 6.00$	0.002	<0.001	0.009	0.002	0.004	0.002	0.010

difference in the value of $\mathcal{A}_{CP}$ using these two fits is assigned as the uncertainty. The fit is also repeated using a reduced mass range of $5.17 < m_{K\mu\mu} < 5.60\ \mathrm{GeV}/c^2$ to investigate the effect of excluding the partially reconstructed background. The difference in results obtained by modeling the combinatorial background using a second-order polynomial, rather than an exponential function, produces a small systematic uncertainty.

Uncertainties also arise from the assumptions made about the asymmetries in background events. Phenomena beyond the SM could cause the CP asymmetry in $B^+ \to \pi^+\mu^+\mu^-$ decays to be large [24], and so the analysis is performed again for values of $\mathcal{A}_{CP}(B^+ \to \pi^+\mu^+\mu^-) = \pm 0.5$, with the larger of the two deviations in $\mathcal{A}_{CP}(B^+ \to K^+\mu^+\mu^-)$ taken as the systematic uncertainty. As the partially reconstructed background can arise from $B^0 \to K^{*0}\mu^+\mu^-$ decays, the value of $\mathcal{A}_{CP}$ for this source background is taken to be -0.072 [7], the value from the LHCb measurement, neglecting any further CP violation in angular distributions. The difference in the fit result compared to the zero $\mathcal{A}_{CP}$ hypothesis is taken as the systematic uncertainty. Variations in $\mathcal{A}_{CP}(B^+ \to K^+\pi^+\pi^-)$ have a negligible effect on the final result. A summary of the systematic uncertainties is shown in Table I. The value of $\mathcal{A}_{CP}$ calculated by performing the fits on the data set integrated over q^2 is consistent with that from the weighted average of the q^2 bins.

The results for $\mathcal{A}_{CP}$ in each q^2 bin and the weighted average are displayed in Table II, as well as in Fig. 2. The value of the raw asymmetry in $B^+ \to J/\psi K^+$ determined from the fit is -0.016 ± 0.002. The CP asymmetry in $B^+ \to K^+\mu^+\mu^-$ decays is measured to be

$$\mathcal{A}_{CP} = 0.000 \pm 0.033\,(\mathrm{stat}) \pm 0.005\,(\mathrm{syst}) \pm 0.007\,(J/\psi K),$$

where the third uncertainty is due to the uncertainty on the known value of $\mathcal{A}_{CP}(B^+ \to J/\psi K^+)$. This compares with the current world average of -0.05 ± 0.13 [20] and previous measurements, including the dielectron final state [2,4]. This result is consistent with the SM, as well as the $B^0 \to K^{*0}\mu^+\mu^-$ decay mode, and improves the precision of the current world average for the dimuon mode by a factor of 4. With the recent observation of resonant structure in the low-recoil region above the $\psi(2S)$ resonance [27], care should be taken when interpreting the result in this region. Interesting effects due to physics beyond the SM are possible through interference with this resonant structure and could be investigated in a future update of the measurement of $\mathcal{A}_{CP}$.

TABLE II. Values of $\mathcal{A}_{CP}$ and the signal yields in the seven q^2 bins, the weighted average, and their associated uncertainties.

q^2 bin (GeV^2/c^4)	Signal yield	$\mathcal{A}_{CP}$	Statistical uncertainty	Systematic uncertainty
$0.05 < q^2 < 2.00$	164 ± 14	-0.152	0.085	0.008
$2.00 < q^2 < 4.30$	167 ± 14	-0.008	0.094	0.012
$4.30 < q^2 < 8.68$	339 ± 21	0.070	0.067	0.005
$10.09 < q^2 < 12.86$	221 ± 17	0.060	0.081	0.024
$14.18 < q^2 < 16.00$	145 ± 13	-0.079	0.091	0.008
$16.00 < q^2 < 18.00$	145 ± 13	0.100	0.093	0.019
$18.00 < q^2 < 22.00$	120 ± 13	-0.070	0.111	0.016
Weighted average		0.000	0.033	0.005
$1.00 < q^2 < 6.00$	362 ± 21	-0.019	0.061	0.010

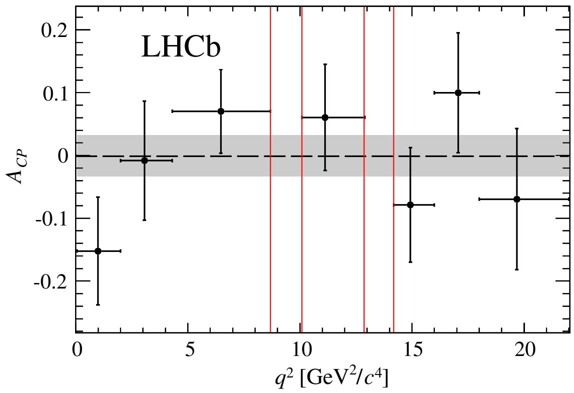

FIG. 2 (color online). Measured value of $\mathcal{A}_{CP}$ in $B^+ \to K^+\mu^+\mu^-$ decays in bins of the $\mu^+\mu^-$ invariant mass squared (q^2). The points are displayed at the mean value of q^2 in each bin. The uncertainties on each $\mathcal{A}_{CP}$ value are the statistical and systematic uncertainties added in quadrature. The excluded charmonium regions are represented by the vertical red lines, the dashed line is the weighted average, and the gray band indicates the 1σ uncertainty on the weighted average.

We express our gratitude to our colleagues in the CERN accelerator departments for the excellent performance of the LHC. We thank the technical and administrative staff at the LHCb institutes. We acknowledge support from CERN and from the national agencies: CAPES, CNPq, FAPERJ, and FINEP (Brazil); NSFC (China); CNRS/IN2P3 and Region Auvergne (France); BMBF, DFG, HGF, and MPG (Germany); SFI (Ireland); INFN (Italy); FOM and NWO (Netherlands); SCSR (Poland); MEN/IFA (Romania); MinES, Rosatom, RFBR, and NRC "Kurchatov Institute" (Russia); MinECo, XuntaGal, and GENCAT (Spain); SNSF and SER (Switzerland); NAS Ukraine (Ukraine); STFC (United Kingdom); and NSF (U.S.A.). We also acknowledge the support received from the ERC under FP7. The Tier1 computing centers are supported by IN2P3 (France), KIT and BMBF (Germany), INFN (Italy), NWO and SURF (Netherlands), PIC (Spain), and GridPP (United Kingdom). We are thankful for the computing resources put at our disposal by Yandex LLC (Russia), as well as to the communities behind the multiple open source software packages that we depend on.

[1] R. Aaij *et al.* (LHCb Collaboration), J. High Energy Phys. 02 (2013) 105.
[2] J.-T. Wei *et al.* (Belle Collaboration), Phys. Rev. Lett. **103**, 171801 (2009).
[3] T. Aaltonen *et al.* (CDF Collaboration), Phys. Rev. Lett. **108**, 081807 (2012).
[4] J. P. Lees *et al.* (*BABAR* Collaboration), Phys. Rev. D **86**, 032012 (2012).
[5] C. Bobeth, G. Hiller, D. van Dyk, and C. Wacker, J. High Energy Phys. 01 (2012) 107.
[6] W. Altmannshofer, P. Ball, A. Bharucha, A. J. Buras, D. M. Straub, and M. Wick, J. High Energy Phys. 01 (2009) 019.
[7] R. Aaij *et al.* (LHCb Collaboration), Phys. Rev. Lett. **110**, 031801 (2013).
[8] A. A. Alves, Jr. *et al.* (LHCb Collaboration), JINST **3**, S08005 (2008).
[9] M. Adinolfi *et al.*, Eur. Phys. J. C **73**, 2431 (2013).
[10] A. A. Alves, Jr. *et al.*, JINST **8**, P02022 (2013).
[11] T. Sjöstrand, S. Mrenna, and P. Skands, J. High Energy Phys. 05 (2006) 026.
[12] I. Belyaev *et al.*, in *Proceedings of the Nuclear Science Symposium Conference Record (NSS/MIC), 2010* (IEEE, New York, 2010), p. 1155.
[13] D. J. Lange, Nucl. Instrum. Methods Phys. Res., Sect. A **462**, 152 (2001).
[14] P. Golonka and Z. Was, Eur. Phys. J. C **45**, 97 (2006).
[15] J. Allison *et al.* (GEANT4 Collaboration), IEEE Trans. Nucl. Sci. **53**, 270 (2006); S. Agostinelli *et al.* (GEANT4 Collaboration), Nucl. Instrum. Methods Phys. Res., Sect. A **506**, 250 (2003).
[16] M. Clemencic, G. Corti, S. Easo, C. R. Jones, S. Miglioranzi, M. Pappagallo, and P. Robbe, J. Phys. Conf. Ser. **331**, 032023 (2011).
[17] R. Aaij *et al.*, JINST **8**, P04022 (2013).
[18] L. Breiman, J. H. Friedman, R. A. Olshen, and C. J. Stone, *Classification and Regression Trees* (Wadsworth, Belmont, CA, 1984).
[19] R. E. Schapire and Y. Freund, J. Comput. Syst. Sci. **55**, 119 (1997).
[20] J. Beringer *et al.* (Particle Data Group), Phys. Rev. D **86**, 010001 (2012).
[21] V. M. Abazov *et al.* (D0 Collaboration), Phys. Rev. Lett. **100**, 211802 (2008).
[22] P. del Amo Sanchez *et al.* (*BABAR* Collaboration), Phys. Rev. D **82**, 051101 (2010).
[23] H. Albrecht *et al.* (ARGUS Collaboration), Phys. Lett. B **229**, 304 (1989).
[24] T. M. Aliev and M. Savci, Phys. Rev. D **60**, 014005 (1999).
[25] R. Aaij *et al.* (LHCb Collaboration), Phys. Rev. Lett. **111**, 101801 (2013).
[26] T. Skwarnicki, Ph.D. thesis, Institute of Nuclear Physics (Institute of Nuclear Physics Report No. DESY-F31-86-02, 1986).
[27] R. Aaij *et al.* (LHCb Collaboration), Phys. Rev. Lett. **111**, 112003 (2013).

R. Aaij,[40] B. Adeva,[36] M. Adinolfi,[45] C. Adrover,[6] A. Affolder,[51] Z. Ajaltouni,[5] J. Albrecht,[9] F. Alessio,[37] M. Alexander,[50] S. Ali,[40] G. Alkhazov,[29] P. Alvarez Cartelle,[36] A. A. Alves Jr,[24,37] S. Amato,[2] S. Amerio,[21] Y. Amhis,[7] L. Anderlini,[17,f] J. Anderson,[39] R. Andreassen,[56] J. E. Andrews,[57] R. B. Appleby,[53] O. Aquines Gutierrez,[10] F. Archilli,[18] A. Artamonov,[34] M. Artuso,[58] E. Aslanides,[6] G. Auriemma,[24,m] M. Baalouch,[5]

S. Bachmann,[11] J. J. Back,[47] C. Baesso,[59] V. Balagura,[30] W. Baldini,[16] R. J. Barlow,[53] C. Barschel,[37] S. Barsuk,[7] W. Barter,[46] Th. Bauer,[40] A. Bay,[38] J. Beddow,[50] F. Bedeschi,[22] I. Bediaga,[1] S. Belogurov,[30] K. Belous,[34] I. Belyaev,[30] E. Ben-Haim,[8] G. Bencivenni,[18] S. Benson,[49] J. Benton,[45] A. Berezhnoy,[31] R. Bernet,[39] M.-O. Bettler,[46] M. van Beuzekom,[40] A. Bien,[11] S. Bifani,[44] T. Bird,[53] A. Bizzeti,[17,h] P. M. Bjørnstad,[53] T. Blake,[37] F. Blanc,[38] J. Blouw,[11] S. Blusk,[58] V. Bocci,[24] A. Bondar,[33] N. Bondar,[29] W. Bonivento,[15] S. Borghi,[53] A. Borgia,[58] T. J. V. Bowcock,[51] E. Bowen,[39] C. Bozzi,[16] T. Brambach,[9] J. van den Brand,[41] J. Bressieux,[38] D. Brett,[53] M. Britsch,[10] T. Britton,[58] N. H. Brook,[45] H. Brown,[51] I. Burducea,[28] A. Bursche,[39] G. Busetto,[21,q] J. Buytaert,[37] S. Cadeddu,[15] O. Callot,[7] M. Calvi,[20,j] M. Calvo Gomez,[35,n] A. Camboni,[35] P. Campana,[18,37] D. Campora Perez,[37] A. Carbone,[14,c] G. Carboni,[23,k] R. Cardinale,[19,i] A. Cardini,[15] H. Carranza-Mejia,[49] L. Carson,[52] K. Carvalho Akiba,[2] G. Casse,[51] L. Castillo Garcia,[37] M. Cattaneo,[37] Ch. Cauet,[9] R. Cenci,[57] M. Charles,[54] Ph. Charpentier,[37] P. Chen,[3,38] N. Chiapolini,[39] M. Chrzaszcz,[25] K. Ciba,[37] X. Cid Vidal,[37] G. Ciezarek,[52] P. E. L. Clarke,[49] M. Clemencic,[37] H. V. Cliff,[46] J. Closier,[37] C. Coca,[28] V. Coco,[40] J. Cogan,[6] E. Cogneras,[5] P. Collins,[37] A. Comerma-Montells,[35] A. Contu,[15,37] A. Cook,[45] M. Coombes,[45] S. Coquereau,[8] G. Corti,[37] B. Couturier,[37] G. A. Cowan,[49] E. Cowie,[45] D. C. Craik,[47] S. Cunliffe,[52] R. Currie,[49] C. D'Ambrosio,[37] P. David,[8] P. N. Y. David,[40] A. Davis,[56] I. De Bonis,[4] K. De Bruyn,[40] S. De Capua,[53] M. De Cian,[11] J. M. De Miranda,[1] L. De Paula,[2] W. De Silva,[56] P. De Simone,[18] D. Decamp,[4] M. Deckenhoff,[9] L. Del Buono,[8] N. Déléage,[4] D. Derkach,[54] O. Deschamps,[5] F. Dettori,[41] A. Di Canto,[11] H. Dijkstra,[37] M. Dogaru,[28] S. Donleavy,[51] F. Dordei,[11] A. Dosil Suárez,[36] D. Dossett,[47] A. Dovbnya,[42] F. Dupertuis,[38] P. Durante,[37] R. Dzhelyadin,[34] A. Dziurda,[25] A. Dzyuba,[29] S. Easo,[48] U. Egede,[52] V. Egorychev,[30] S. Eidelman,[33] D. van Eijk,[40] S. Eisenhardt,[49] U. Eitschberger,[9] R. Ekelhof,[9] L. Eklund,[50,37] I. El Rifai,[5] Ch. Elsasser,[39] A. Falabella,[14,e] C. Färber,[11] G. Fardell,[49] C. Farinelli,[40] S. Farry,[51] D. Ferguson,[49] V. Fernandez Albor,[36] F. Ferreira Rodrigues,[1] M. Ferro-Luzzi,[37] S. Filippov,[32] M. Fiore,[16] C. Fitzpatrick,[37] M. Fontana,[10] F. Fontanelli,[19,i] R. Forty,[37] O. Francisco,[2] M. Frank,[37] C. Frei,[37] M. Frosini,[17,f] S. Furcas,[20] E. Furfaro,[23,k] A. Gallas Torreira,[36] D. Galli,[14,c] M. Gandelman,[2] P. Gandini,[58] Y. Gao,[3] J. Garofoli,[58] P. Garosi,[53] J. Garra Tico,[46] L. Garrido,[35] C. Gaspar,[37] R. Gauld,[54] E. Gersabeck,[11] M. Gersabeck,[53] T. Gershon,[47,37] Ph. Ghez,[4] V. Gibson,[46] L. Giubega,[28] V. V. Gligorov,[37] C. Göbel,[59] D. Golubkov,[30] A. Golutvin,[52,30,37] A. Gomes,[2] P. Gorbounov,[30,37] H. Gordon,[37] C. Gotti,[20] M. Grabalosa Gándara,[5] R. Graciani Diaz,[35] L. A. Granado Cardoso,[37] E. Graugés,[35] G. Graziani,[17] A. Grecu,[28] E. Greening,[54] S. Gregson,[46] P. Griffith,[44] O. Grünberg,[60] B. Gui,[58] E. Gushchin,[32] Yu. Guz,[34,37] T. Gys,[37] C. Hadjivasiliou,[58] G. Haefeli,[38] C. Haen,[37] S. C. Haines,[46] S. Hall,[52] B. Hamilton,[57] T. Hampson,[45] S. Hansmann-Menzemer,[11] N. Harnew,[54] S. T. Harnew,[45] J. Harrison,[53] T. Hartmann,[60] J. He,[37] T. Head,[37] V. Heijne,[40] K. Hennessy,[51] P. Henrard,[5] J. A. Hernando Morata,[36] E. van Herwijnen,[37] M. Hess,[60] A. Hicheur,[1] E. Hicks,[51] D. Hill,[54] M. Hoballah,[5] C. Hombach,[53] P. Hopchev,[4] W. Hulsbergen,[40] P. Hunt,[54] T. Huse,[51] N. Hussain,[54] D. Hutchcroft,[51] D. Hynds,[50] V. Iakovenko,[43] M. Idzik,[26] P. Ilten,[12] R. Jacobsson,[37] A. Jaeger,[11] E. Jans,[40] P. Jaton,[38] A. Jawahery,[57] F. Jing,[3] M. John,[54] D. Johnson,[54] C. R. Jones,[46] C. Joram,[37] B. Jost,[37] M. Kaballo,[9] S. Kandybei,[42] W. Kanso,[6] M. Karacson,[37] T. M. Karbach,[37] I. R. Kenyon,[44] T. Ketel,[41] A. Keune,[38] B. Khanji,[20] O. Kochebina,[7] I. Komarov,[38] R. F. Koopman,[41] P. Koppenburg,[40] M. Korolev,[31] A. Kozlinskiy,[40] L. Kravchuk,[32] K. Kreplin,[11] M. Kreps,[47] G. Krocker,[11] P. Krokovny,[33] F. Kruse,[9] M. Kucharczyk,[20,25,j] V. Kudryavtsev,[33] K. Kurek,[27] T. Kvaratskheliya,[30,37] V. N. La Thi,[38] D. Lacarrere,[37] G. Lafferty,[53] A. Lai,[15] D. Lambert,[49] R. W. Lambert,[41] E. Lanciotti,[37] G. Lanfranchi,[18] C. Langenbruch,[37] T. Latham,[47] C. Lazzeroni,[44] R. Le Gac,[6] J. van Leerdam,[40] J.-P. Lees,[4] R. Lefèvre,[5] A. Leflat,[31] J. Lefrançois,[7] S. Leo,[22] O. Leroy,[6] T. Lesiak,[25] B. Leverington,[11] Y. Li,[3] L. Li Gioi,[5] M. Liles,[51] R. Lindner,[37] C. Linn,[11] B. Liu,[3] G. Liu,[37] S. Lohn,[37] I. Longstaff,[50] J. H. Lopes,[2] N. Lopez-March,[38] H. Lu,[3] D. Lucchesi,[21,q] J. Luisier,[38] H. Luo,[49] F. Machefert,[7] I. V. Machikhiliyan,[4,30] F. Maciuc,[28] O. Maev,[29,37] S. Malde,[54] G. Manca,[15,d] G. Mancinelli,[6] J. Maratas,[5] U. Marconi,[14] P. Marino,[22,s] R. Märki,[38] J. Marks,[11] G. Martellotti,[24] A. Martens,[8] A. Martín Sánchez,[7] M. Martinelli,[40] D. Martinez Santos,[41] D. Martins Tostes,[2] A. Martynov,[31] A. Massafferri,[1] R. Matev,[37] Z. Mathe,[37] C. Matteuzzi,[20] E. Maurice,[6] A. Mazurov,[16,32,37,e] J. McCarthy,[44] A. McNab,[53] R. McNulty,[12] B. McSkelly,[51] B. Meadows,[56,54] F. Meier,[9] M. Meissner,[11] M. Merk,[40] D. A. Milanes,[8] M.-N. Minard,[4] J. Molina Rodriguez,[59] S. Monteil,[5] D. Moran,[53] P. Morawski,[25] A. Mordà,[6] M. J. Morello,[22,s] R. Mountain,[58] I. Mous,[40] F. Muheim,[49] K. Müller,[39] R. Muresan,[28] B. Muryn,[26] B. Muster,[38] P. Naik,[45] T. Nakada,[38] R. Nandakumar,[48] I. Nasteva,[1] M. Needham,[49] S. Neubert,[37] N. Neufeld,[37] A. D. Nguyen,[38] T. D. Nguyen,[38] C. Nguyen-Mau,[38,o] M. Nicol,[7] V. Niess,[5] R. Niet,[9] N. Nikitin,[31] T. Nikodem,[11] A. Nomerotski,[54] A. Novoselov,[34] A. Oblakowska-Mucha,[26] V. Obraztsov,[34] S. Oggero,[40] S. Ogilvy,[50] O. Okhrimenko,[43] R. Oldeman,[15,d]

M. Orlandea,[28] J. M. Otalora Goicochea,[2] P. Owen,[52] A. Oyanguren,[35] B. K. Pal,[58] A. Palano,[13,b] T. Palczewski,[27] M. Palutan,[18] J. Panman,[37] A. Papanestis,[48] M. Pappagallo,[50] C. Parkes,[53] C. J. Parkinson,[52] G. Passaleva,[17] G. D. Patel,[51] M. Patel,[52] G. N. Patrick,[48] C. Patrignani,[19,i] C. Pavel-Nicorescu,[28] A. Pazos Alvarez,[36] A. Pellegrino,[40] G. Penso,[24,l] M. Pepe Altarelli,[37] S. Perazzini,[14,c] E. Perez Trigo,[36] A. Pérez-Calero Yzquierdo,[35] P. Perret,[5] M. Perrin-Terrin,[6] L. Pescatore,[44] E. Pesen,[61] K. Petridis,[52] A. Petrolini,[19,i] A. Phan,[58] E. Picatoste Olloqui,[35] B. Pietrzyk,[4] T. Pilař,[47] D. Pinci,[24] S. Playfer,[49] M. Plo Casasus,[36] F. Polci,[8] G. Polok,[25] A. Poluektov,[47,33] E. Polycarpo,[2] A. Popov,[34] D. Popov,[10] B. Popovici,[28] C. Potterat,[35] A. Powell,[54] J. Prisciandaro,[38] A. Pritchard,[51] C. Prouve,[7] V. Pugatch,[43] A. Puig Navarro,[38] G. Punzi,[22,r] W. Qian,[4] J. H. Rademacker,[45] B. Rakotomiaramanana,[38] M. S. Rangel,[2] I. Raniuk,[42] N. Rauschmayr,[37] G. Raven,[41] S. Redford,[54] M. M. Reid,[47] A. C. dos Reis,[1] S. Ricciardi,[48] A. Richards,[52] K. Rinnert,[51] V. Rives Molina,[35] D. A. Roa Romero,[5] P. Robbe,[7] D. A. Roberts,[57] E. Rodrigues,[53] P. Rodriguez Perez,[36] S. Roiser,[37] V. Romanovsky,[34] A. Romero Vidal,[36] J. Rouvinet,[38] T. Ruf,[37] F. Ruffini,[22] H. Ruiz,[35] P. Ruiz Valls,[35] G. Sabatino,[24,k] J. J. Saborido Silva,[36] N. Sagidova,[29] P. Sail,[50] B. Saitta,[15,d] V. Salustino Guimaraes,[2] B. Sanmartin Sedes,[36] M. Sannino,[19,i] R. Santacesaria,[24] C. Santamarina Rios,[36] E. Santovetti,[23,k] M. Sapunov,[6] A. Sarti,[18,l] C. Satriano,[24,m] A. Satta,[23] M. Savrie,[16,e] D. Savrina,[30,31] P. Schaack,[52] M. Schiller,[41] H. Schindler,[37] M. Schlupp,[9] M. Schmelling,[10] B. Schmidt,[37] O. Schneider,[38] A. Schopper,[37] M.-H. Schune,[7] R. Schwemmer,[37] B. Sciascia,[18] A. Sciubba,[24] M. Seco,[36] A. Semennikov,[30] K. Senderowska,[26] I. Sepp,[52] N. Serra,[39] J. Serrano,[6] P. Seyfert,[11] M. Shapkin,[34] I. Shapoval,[16,42] P. Shatalov,[30] Y. Shcheglov,[29] T. Shears,[51,37] L. Shekhtman,[33] O. Shevchenko,[42] V. Shevchenko,[30] A. Shires,[9] R. Silva Coutinho,[47] M. Sirendi,[46] N. Skidmore,[45] T. Skwarnicki,[58] N. A. Smith,[51] E. Smith,[54,48] J. Smith,[46] M. Smith,[53] M. D. Sokoloff,[56] F. J. P. Soler,[50] F. Soomro,[38] D. Souza,[45] B. Souza De Paula,[2] B. Spaan,[9] A. Sparkes,[49] P. Spradlin,[50] F. Stagni,[37] S. Stahl,[11] O. Steinkamp,[39] S. Stevenson,[54] S. Stoica,[28] S. Stone,[58] B. Storaci,[39] M. Straticiuc,[28] U. Straumann,[39] V. K. Subbiah,[37] L. Sun,[56] S. Swientek,[9] V. Syropoulos,[41] M. Szczekowski,[27] P. Szczypka,[38,37] T. Szumlak,[26] S. T'Jampens,[4] M. Teklishyn,[7] E. Teodorescu,[28] F. Teubert,[37] C. Thomas,[54] E. Thomas,[37] J. van Tilburg,[11] V. Tisserand,[4] M. Tobin,[38] S. Tolk,[41] D. Tonelli,[37] S. Topp-Joergensen,[54] N. Torr,[54] E. Tournefier,[4,52] S. Tourneur,[38] M. T. Tran,[38] M. Tresch,[39] A. Tsaregorodtsev,[6] P. Tsopelas,[40] N. Tuning,[40] M. Ubeda Garcia,[37] A. Ukleja,[27] D. Urner,[53] A. Ustyuzhanin,[52,p] U. Uwer,[11] V. Vagnoni,[14] G. Valenti,[14] A. Vallier,[7] M. Van Dijk,[45] R. Vazquez Gomez,[18] P. Vazquez Regueiro,[36] C. Vázquez Sierra,[36] S. Vecchi,[16] J. J. Velthuis,[45] M. Veltri,[17,g] G. Veneziano,[38] M. Vesterinen,[37] B. Viaud,[7] D. Vieira,[2] X. Vilasis-Cardona,[35,n] A. Vollhardt,[39] D. Volyanskyy,[10] D. Voong,[45] A. Vorobyev,[29] V. Vorobyev,[33] C. Voß,[60] H. Voss,[10] R. Waldi,[60] C. Wallace,[47] R. Wallace,[12] S. Wandernoth,[11] J. Wang,[58] D. R. Ward,[46] N. K. Watson,[44] A. D. Webber,[53] D. Websdale,[52] M. Whitehead,[47] J. Wicht,[37] J. Wiechczynski,[25] D. Wiedner,[11] L. Wiggers,[40] G. Wilkinson,[54] M. P. Williams,[47,48] M. Williams,[55] F. F. Wilson,[48] J. Wimberley,[57] J. Wishahi,[9] W. Wislicki,[27] M. Witek,[25] S. A. Wotton,[46] S. Wright,[46] S. Wu,[3] K. Wyllie,[37] Y. Xie,[49,37] Z. Xing,[58] Z. Yang,[3] R. Young,[49] X. Yuan,[3] O. Yushchenko,[34] M. Zangoli,[14] M. Zavertyaev,[10,a] F. Zhang,[3] L. Zhang,[58] W. C. Zhang,[12] Y. Zhang,[3] A. Zhelezov,[11] A. Zhokhov,[30] L. Zhong,[3] and A. Zvyagin[37]

(LHCb Collaboration)

[1]*Centro Brasileiro de Pesquisas Físicas (CBPF), Rio de Janeiro, Brazil*
[2]*Universidade Federal do Rio de Janeiro (UFRJ), Rio de Janeiro, Brazil*
[3]*Center for High Energy Physics, Tsinghua University, Beijing, China*
[4]*LAPP, Université de Savoie, CNRS/IN2P3, Annecy-Le-Vieux, France*
[5]*Clermont Université, Université Blaise Pascal, CNRS/IN2P3, LPC, Clermont-Ferrand, France*
[6]*CPPM, Aix-Marseille Université, CNRS/IN2P3, Marseille, France*
[7]*LAL, Université Paris-Sud, CNRS/IN2P3, Orsay, France*
[8]*LPNHE, Université Pierre et Marie Curie, Université Paris Diderot, CNRS/IN2P3, Paris, France*
[9]*Fakultät Physik, Technische Universität Dortmund, Dortmund, Germany*
[10]*Max-Planck-Institut für Kernphysik (MPIK), Heidelberg, Germany*
[11]*Physikalisches Institut, Ruprecht-Karls-Universität Heidelberg, Heidelberg, Germany*
[12]*School of Physics, University College Dublin, Dublin, Ireland*
[13]*Sezione INFN di Bari, Bari, Italy*
[14]*Sezione INFN di Bologna, Bologna, Italy*
[15]*Sezione INFN di Cagliari, Cagliari, Italy*
[16]*Sezione INFN di Ferrara, Ferrara, Italy*

[17]*Sezione INFN di Firenze, Firenze, Italy*
[18]*Laboratori Nazionali dell'INFN di Frascati, Frascati, Italy*
[19]*Sezione INFN di Genova, Genova, Italy*
[20]*Sezione INFN di Milano Bicocca, Milano, Italy*
[21]*Sezione INFN di Padova, Padova, Italy*
[22]*Sezione INFN di Pisa, Pisa, Italy*
[23]*Sezione INFN di Roma Tor Vergata, Roma, Italy*
[24]*Sezione INFN di Roma La Sapienza, Roma, Italy*
[25]*Henryk Niewodniczanski Institute of Nuclear Physics, Polish Academy of Sciences, Kraków, Poland*
[26]*AGH University of Science and Technology, Faculty of Physics and Applied Computer Science, Kraków, Poland*
[27]*National Center for Nuclear Research (NCBJ), Warsaw, Poland*
[28]*Horia Hulubei National Institute of Physics and Nuclear Engineering, Bucharest-Magurele, Romania*
[29]*Petersburg Nuclear Physics Institute (PNPI), Gatchina, Russia*
[30]*Institute of Theoretical and Experimental Physics (ITEP), Moscow, Russia*
[31]*Institute of Nuclear Physics, Moscow State University (SINP MSU), Moscow, Russia*
[32]*Institute for Nuclear Research of the Russian Academy of Sciences (INR RAN), Moscow, Russia*
[33]*Budker Institute of Nuclear Physics (SB RAS) and Novosibirsk State University, Novosibirsk, Russia*
[34]*Institute for High Energy Physics (IHEP), Protvino, Russia*
[35]*Universitat de Barcelona, Barcelona, Spain*
[36]*Universidad de Santiago de Compostela, Santiago de Compostela, Spain*
[37]*European Organization for Nuclear Research (CERN), Geneva, Switzerland*
[38]*Ecole Polytechnique Fédérale de Lausanne (EPFL), Lausanne, Switzerland*
[39]*Physik-Institut, Universität Zürich, Zürich, Switzerland*
[40]*Nikhef National Institute for Subatomic Physics, Amsterdam, Netherlands*
[41]*Nikhef National Institute for Subatomic Physics and VU University Amsterdam, Amsterdam, Netherlands*
[42]*NSC Kharkiv Institute of Physics and Technology (NSC KIPT), Kharkiv, Ukraine*
[43]*Institute for Nuclear Research of the National Academy of Sciences (KINR), Kyiv, Ukraine*
[44]*University of Birmingham, Birmingham, United Kingdom*
[45]*H.H. Wills Physics Laboratory, University of Bristol, Bristol, United Kingdom*
[46]*Cavendish Laboratory, University of Cambridge, Cambridge, United Kingdom*
[47]*Department of Physics, University of Warwick, Coventry, United Kingdom*
[48]*STFC Rutherford Appleton Laboratory, Didcot, United Kingdom*
[49]*School of Physics and Astronomy, University of Edinburgh, Edinburgh, United Kingdom*
[50]*School of Physics and Astronomy, University of Glasgow, Glasgow, United Kingdom*
[51]*Oliver Lodge Laboratory, University of Liverpool, Liverpool, United Kingdom*
[52]*Imperial College London, London, United Kingdom*
[53]*School of Physics and Astronomy, University of Manchester, Manchester, United Kingdom*
[54]*Department of Physics, University of Oxford, Oxford, United Kingdom*
[55]*Massachusetts Institute of Technology, Cambridge, Massachusetts, USA*
[56]*University of Cincinnati, Cincinnati, Ohio, USA*
[57]*University of Maryland, College Park, Maryland, USA*
[58]*Syracuse University, Syracuse, New York, USA*
[59]*Pontifícia Universidade Católica do Rio de Janeiro (PUC-Rio), Rio de Janeiro, Brazil [associated with Universidade Federal do Rio de Janeiro (UFRJ), Rio de Janeiro, Brazil]*
[60]*Institut für Physik, Universität Rostock, Rostock, Germany (associated with Physikalisches Institut, Ruprecht-Karls-Universität Heidelberg, Heidelberg, Germany)*
[61]*Celal Bayar University, Manisa, Turkey [associated with European Organization for Nuclear Research (CERN), Geneva, Switzerland]*

[a]Also at P. N. Lebedev Physical Institute, Russian Academy of Science (LPI RAS), Moscow, Russia.
[b]Also at Università di Bari, Bari, Italy.
[c]Also at Università di Bologna, Bologna, Italy.
[d]Also at Università di Cagliari, Cagliari, Italy.
[e]Also at Università di Ferrara, Ferrara, Italy.
[f]Also at Università di Firenze, Firenze, Italy.
[g]Also at Università di Urbino, Urbino, Italy.
[h]Also at Università di Modena e Reggio Emilia, Modena, Italy.
[i]Also at Università di Genova, Genova, Italy.
[j]Also at Università di Milano Bicocca, Milano, Italy.
[k]Also at Università di Roma Tor Vergata, Roma, Italy.

[l]Also at Università di Roma La Sapienza, Roma, Italy.
[m]Also at Università della Basilicata, Potenza, Italy.
[n]Also at LIFAELS, La Salle, Universitat Ramon Llull, Barcelona, Spain.
[o]Also at Hanoi University of Science, Hanoi, Vietnam.
[p]Also at Institute of Physics and Technology, Moscow, Russia.
[q]Also at Università di Padova, Padova, Italy.
[r]Also at Università di Pisa, Pisa, Italy.
[s]Also at Scuola Normale Superiore, Pisa, Italy.